ATMOSPHERIC CORRECTION OF SATELLITE IMAGERY USING MODTRAN 3.5 CODE*

Fabián O. González and Miguel Vélez-Reyes
Advanced Automated Image Processing Project
Tropical Center for Earth and Space Studies
University of Puerto Rico-Mayagüez
Mayagüez, Puerto Rico 00681
Tel, (787) 832-4040, x3086, 3094 Fax. (787) 831-7564
e-mail: fabiang@exodo.upr.clu.edu   mvelez@exodo.upr.clu.edu

Abstract—When performing satellite remote sensing of the earth in the solar spectrum, atmospheric scattering and absorption effects provide the sensors corrupted information about the target's radiance characteristics. We are faced with the problem of reconstructing the signal that was reflected from the target, from the data sensed by the remote sensing instrument. This article presents a method for simulating radiance characteristic curves of satellite images using a MODTRAN 3.5 band model (BM) code to solve the radiative transfer equation (RTE), and proposes a method for the implementation of an adaptive system for automated atmospheric corrections. The simulation procedure is carried out as follows: (1) for each satellite digital image a radiance characteristic curve is obtained by performing a digital number (DN) to radiance conversion, (2) using MODTRAN 3.5 a simulation of the images characteristic curves is generated, (3) the output of the code is processed to generate radiance characteristic curves for the simulated cases. The simulation algorithm was used to simulate Landsat Thematic Mapper (TM) images for two types of locations: the ocean surface, and a forest surface. The simulation procedure was validated by computing the error between the empirical and simulated radiance curves. While results in the visible region of the spectrum where not very accurate, those for the infrared region of the spectrum were encouraging. This information can be used for correction of the atmospheric effects. For the simulation over ocean, the lowest error produced in this region was of the order of 10^{-5} and up to 14 times smaller than errors in the visible region. For the same spectral region on the forest case, the lowest error produced was of the order of 10-4, and up to 41 times smaller than errors in the visible region,

1. INTRODUCTION

In the solar spectrum, sensors on Earth remote sensing satellites measure the radiance reflected by the atmosphere-Earth surface system illuminated by the sun. While this signal depends on the surface reflectance, it is perturbed significantly by two atmospheric processes, the gaseous absorption and the scattering by molecules and aerosols[1]. Atmospheric molecules and aerosols can modulate the radiation reflected from the earth by attenuating it, changing its spatial distribution, and introducing into the field of view, radiation from sunlight scattered in the atmosphere This provides the sensor, corrupted information about the target's radiance characteristics, resulting in blurred images or altered contrasts in image colors. We arc faced with the problem of reconstructing the signal that was reflected from the target from the data sensed by the remote sensing instrument. This is not generally a simple process due to the spatial and temporal dependence of the atmospheric effects.

Simulation of satellite imagery is a powerful tool that can be used effectively in the development and implementation of preprocessing techniques on the digital data. Results from simulations of sensor measured radiance can be used in the development of atmospheric correction algorithms to be applied to satellite data, Our goal in this research is the development of an adaptive system for automated atmospheric corrections of the digital data. The information obtained from the simulation (i.e., from the solution of the RTE) provides an estimation of the corrected radiance. This problem can be treated as a filtering system (see Figure 1). The spatial and temporal variability of atmospheric effects suggests the study of adaptive systems and approaches to on-line adaptation of atmospheric models used in atmospheric corrections. The estimated surface reflectance extracted from the radiation received at the sensor, can be processed by some adaptation mechanism to estimate the atmospheric parameters and readapt the model for new computations of the RTE. The automated and adaptive nature of this system should make it a powerful one.

We selected a Landsat TM satellite image with no atmospheric corrections, to simulate its spectral radiance characteristic. TM images contain digital data for seven channels or spectral bands located in different atmospheric windows (see Table 1). This gives us information about the radiance in the visible region of the spectrum, and the near, mid, and thermal infrared. We selected two surfaces with known reflectance characteristics to simulate: a forest, and the ocean. The simulations were carried out using MODTRAN 3.5, This is a computer code based in a subroutine of the equation of radiative transfer, capable of making calculations of atmospheric transmittance or radiance at a mid spectral resolutions. The code was developed by researchers from Phillips Laboratory, at Hanscom Air Force Base in Boston. Massachusetts.

2. PROCEDURE

Using a computer software for image processing, we obtained the digital number (DN) for a single pixel in each of the surfaces, and for each channel. We collected seven DN values for each surface, i.e., one value for each channel. Conversion from the DN of TM digital data to at-satellite spectral radiance was done using calibration data supplied by EOSAT. After this conversion was performed, we had seven radiance values for each scene simulated. One value for each one of the TM channels, Plotting these values against the central wavelength of the sensors' bandwidths, we obtained measured radiance curves for surfaces of forest and ocean.

We executed MODTRAN 3,5 setting the input parameters to simulate the surface, atmospheric, and geometry characteristics of the real system. By executing the program we obtained top-of-the-atmosphere (TOA) spectral radiance, or at-satellite spectral radiance, for a spectral band from 0.4μm to 12.5 μm. We compared the curves obtained using MODTRAN 3.5 with those obtained from the TM digital data.

Table 1 Atmospheric Windows for Terrestrial Observations by Satellites

Spectral Region	Atmospheric Window (pm}	TM Sensor Band(μm)
Visible	(between) 0.4-0.75	band 1:0.45-0,52
		band 3:0.63-0.69
Near Infrared	(at about) 0.85	band 4:0.76-0.90
Middle Infrared	(at about) 1.06, 1.22, 1.60	band 5:1.55-1.75
	(at about) 2.20	band 7:2.08-2.35
Thermal Infrared	(at about) 4.00, 11.00	band 6:10.40-12.50

We can summarize this procedure in the following steps:

1. Select an appropriate satellite image in digital data. We will use pixels from this image for the simulation.
2. Select a number of pixels in the image with known reflectivity and emissivity characteristics, which correspond to different type of surfaces, one pixel per type of surface to be used in the simulation.
3. Obtain the digital numbers (DN) for each selected pixel.
4. Repeat step 3 for each channel available in the digital data.
5. Convert each of the DN values to spectral radiance values.
6. Run the MODTRAN 3.5 simulation, setting the input parameters so that they match as close as possible, the digital data used for the simulation.
7. Compute the average radiance for the spectral range that corresponds to each of the satellite sensors,
8. Plot these average values against wavelength, using the center wavelength of each spectral band,
9. Repeat steps 8 through 10 for each case emulated.
10. Plot the converted DN to radiance values from the digital data, using the same wavelength axis as in MODTRAN plots.
11. Calculate the error between both sets of graphs.

3. EVALUATION OF RESULTS

3.1. *DN to Radiance Conversion of the TM Digital Data*

The curves corresponding to the DN to radiance conversion of the ocean and forest surfaces are plotted in Figure 2a and 2b, respectively. Knowing that a change in DN implies a change in radiance, we can see how this radiometric quantity varies with wavelength in each selected surface.

Looking at the curve for the ocean surface, we would expect water to show high absorption in the near and mid-IR spectral region[4]. This is probably the most distinctive reflectance characteristic of water. We can see from Figure 2a, that at these wavelengths the lowest radiance values (and generally lower DN values) are recorded. Atmospheric scattering and absorption effects are mostly present in the visible region of the region of the spectrums. The curve for the forest surface differs greatly from the curve for ocean in the visible region of the spectrum. In the next section we will see how the simulation helps us in the analysis and interpretation of the DN to radiance conversion curves, especially in this spectral region.

3.2. MODTRAN 3.5 Simulation

MODTRAN simulates the most important radiance characteristics for a given atmosphere-Earth system. These are: atmospheric transmittance, optical depth, path thermal radiance, surface emission, total path scattered radiance, ground reflected radiance, and total radiance[6]. We will limit our discussion to the total radiance and the ground reflected plus surface emitted radiance. This will suffice to show the dramatic effects of atmospheric absorption and scattering in solar radiance, and to show how the simulations provide a great deal of information to be used when developing correcting tools.

The curves of the ground reflected plus surface emitted radiance are plotted in Figure 3a and 3b, for ocean and forest respectively. These curves approximate what we would receive at the satellite sensor if scattering effects where not present. The ground reflected radiance is constituted by a direct reflection term and a scattered reflected term. The direct ground reflected includes the directly transmitted solar radiance reaching the ground, whereas the scattered term is the solar radiation scattered within the atmosphere before reaching the ground. This scattering effect is increased in the visible region of the spectrum.

Now knowing what is the desired response, let us take a look at the curves of the total radiance in Figures 4a and 4b. We would like to eliminate the scattered ground reflected radiance, path scattered radiance, and path emitted radiance. The fact is that these terms are included in the total radiance. Thus, in the figure, instead of having a measurement of true surface reflected and emitted radiance, we have obtained a false or apparent radiance'. This leads to an altered or apparent reflectance characteristic of the sensed surface. We have to mention that the molecular absorption effects have been diminished by measuring the radiance in adequate atmospheric windows. Still, we are not dealing in any way with the measurement of aerosol absorption effects,

The difference between the total radiance measurement and the ground reflected and emitted radiance is shown in Figures 5a and 5b.

3.3. *Mean Radiance Values for Spectral Bands Corresponding to TM Channels*

The purpose of' calculating the mean radiance for seven spectral bands is to approximate the radiance measurements as they would be obtained with the Landsat TM sensors. To do this, we are assuming that the radiance measured by one of the TM sensors is the average value of the point of interest plus the values of its neighbors. Thus, by calculating the mean radiance value over the selected spectral bands, we will be simulating the total radiance measured by the sensors. We also assume that this measured radiance corresponds to the center wavelength of each spectral band.

Figures 6a and 6b contain the mean values for the ground reflected plus surface emitted radiance. Figures 7a and 7b show the mean total radiance per channel calculated from the simulation. Figures 6 and 7 derive from Figures 3 and 4, respective] y. The difference **between** Figures 6 and 7 is the undesired radiance introduced by the atmospheric effects.

3.4. *Comparing the empirical and simulation results*

We compare the results based on the error between plots for DN to radiance conversion and mean values calculations for total radiance, i.e., the difference between Figures 2 and 7. The curve in Figure 8a is the error produced *in* the simulation of the ocean surface. From this figure we see that the minimum error occurs for channel 7 in the mid-infrared (2.08 -2.35 pm), and it is of the order of 10-5. The maximum error occurs in channel 3 (red, 0.63- 0.69 μm) in the visible region. This error is of the order of 10^{-4}. Exacty, the error in channel 3 is 14 times higher than the error in channel 7. In general, the error in the visible region of the spectrum will be the highest. We can mention a set of factors that could influence the outcome of this simulation.

We know that scattering effects are more critical within the visible region of the spectrum. The measured radiance will depend, to a high extent, on the atmospheric characteristics of the radiance path. In other words, there will be a significant component of the total radiation that will always vary according to the location where a certain surface is sensed. This alone introduces a high degree of uncertainty, The simulation errors can be minimized by using atmospheric and surface models which are representative of the surface to be simulated, and of the atmosphere

over that surface. We cannot have general models that work all the times, especially within the visible region of the spectrum. This addresses the issue of an adaptive correction system.

Since the total radiance of the simulation approximates the empirical results, we can estimate the correct radiance in the image by subtracting the difference between Figures 6 and 7 from Figure 2. Conceptually, we can use the surface and atmospheric parameters generated by the simulation to implement an adaptation mechanism for the correction of the measured radiance (Figure 1).

Figure 8b presents the error in the simulation of the forest surface, Maximum and minimum errors occur in the visible and thermal-IR respectively. We would expect the radiance in the blue and red portions of the spectrum to be lower than radiance in the green channel. Looking at Figure 8b we will notice the peak in the blue channel corresponding to TM channel 1. The reason for this might reside on the selection of reflectivity and emissivity for forest. The available forest reflectivity and emissivity values may not be representative of the type of forest sensed in the image. The chlorophyll content of the plant leaves will affect the reflectivity in the visible region of the spectrum. Thus, reflectivity in the visible may vary greatly as the type of vegetation that grows in a particular forest changes[4].

For wavelengths in the infrared, the error between the radiance magnitudes for a particular wavelength is much smaller than the error for wavelengths in the visible. We see from the errors in channels one and seven that the error corresponding to the blue spectral region (0.45 -0.52 µm) is 41 times higher than the error in the thermal-IR, where the error is of the the order of 10-4. The small errors in the IR region indicate the existing similarity between the image and the simulation, not only in the proportionality within each case, but also in the magnitude of the values.

4. SUMMARY AND CONCLUSIONS

We have presented a simple but useful method for the simulation of solar radiance, and its potential applications to the correction of atmospheric effects in satellite imagery. By simulating effects of scattering and absorption in solar radiance, atmospheric and surface parameters can be obtained that can be used to estimate correct surface radiance. Simulations based on the radiative transfer equation (RTE) can be used to estimate radiance values to be compared to values measured by satellite sensors. The error between these values can be used in some adaptation mechanism, which will generate new atmospheric and surface parameters to adapt the model for new radiative transfer computations.

We used MODTRAN 3.5, a code based on a subroutine of the RTE to simulate radiance characteristics of ocean and forest surfaces in Landsat Thematic 'Mapper (TM) digital data. In general, higher errors between the simulated and measured values were obtained in the visible region of the spectrum, due to greater atmospheric scattering in this spectral region. Within the spectral range from near-IR to far-IR, results of the simulation were very encouraging. For the ocean surface, simulation errors in the visible region of the spectrum were up to 14 times higher than errors in the IR spectrum, were the minimum errors were of the order of 10^{-5}. For the forest surface, errors were of the order of 10"4 on the IR region, and errors in the visible region were op to 41 times higher.

The simulation process still needs to be fine tuned. Uncertainty factors must be minimized to assure the accuracy of the simulations, especially in the visible region of the spectrum. This can be clone by adding to the simulation code, atmospheric and surface data that models more accurately the real case. Also, we need to address computational issues. The procedure developed is applied in a pixel by pixel basis. Application of this procedure on blocks of pixels in an image, must take into consideration the implementation of some architecture to perform parallel processing of the pixels.

5, REFERENCES

1. Vermote E., Tanré D., Deuzé J. L., Herman M., and Morcrette J.J. **Second Simulation of the Satellite Signal in the Solar Spectrum (6 S).** Laboratoire d'Optique Atmosphérique, Université des Sciences et Technologies de Line, Line, France, 216 pp.
2. Asrar, G. 1993. Theory **and Applications of Optical** Remote Sensing. John Wiley and Sons, New York, USA, 730 pp.
3. Berk, A., L.S. Bernstein, D.C. Robertson, 1989, **MODTRAN: A** Moderate Resolution **Model** for **LOWTRAN** 7. Phillips Laboratory, Hanscom US Air Force Base, 38 pp.
4. Lillesand, T.M., and R.W. Kiefer. Remote Sensing and Image Interpretation. John Wiley& Sons, NY, USA.
5. Lenoble, J. Atmospheric Radiative Transfer. A. DEEPAK Publishing, Hampton, Virginia USA, 532 pp.
6. Berk, A., L.S. Bernstein, D.C. Robertson, 1995. **MODTRAN** 3 User Instructions. Phillips Laboratories, Hanscom US Air Force Base, 38 pp.
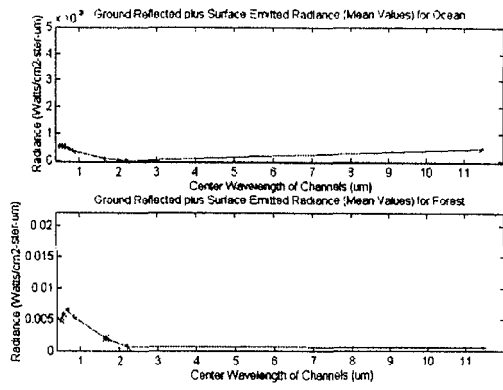
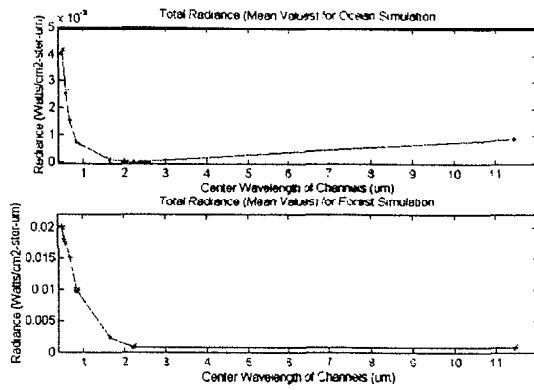**Figure 6 Channel Mean Values for Ground Reflected plus emitted radiance**
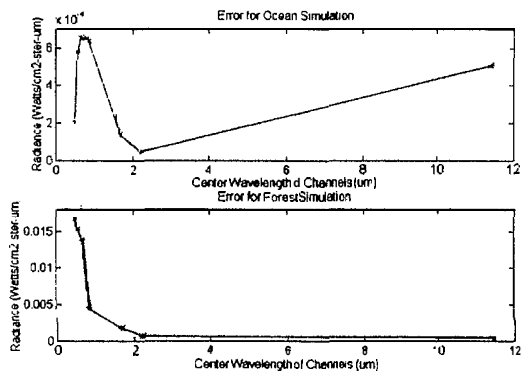

Figure 7 Channel Mean Values for Total Radiance

Figure 8 Final error for simulated cases
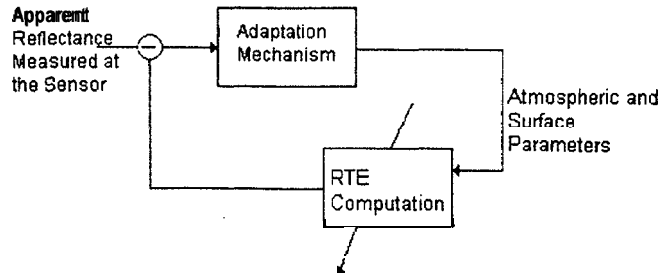
289

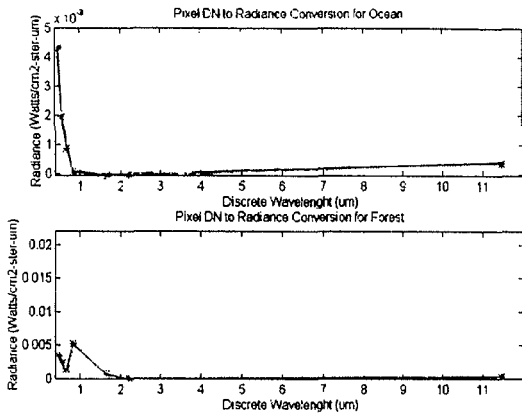**Figure 1 Model of an adaptive system for automated atmospheric corrections**

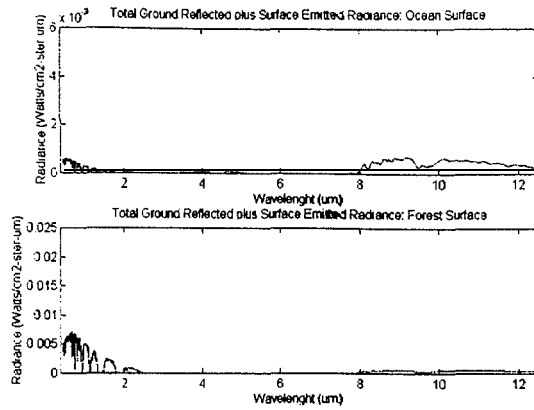Figure 2 DN to Radiance Conversions

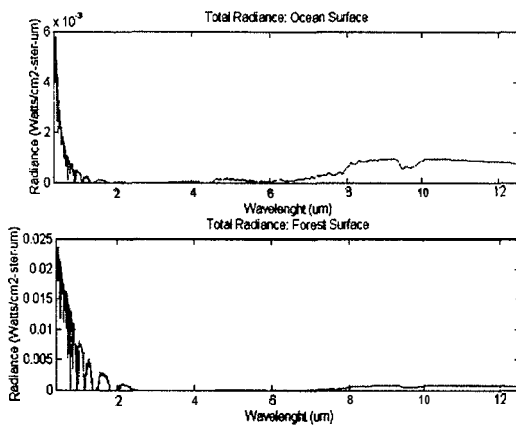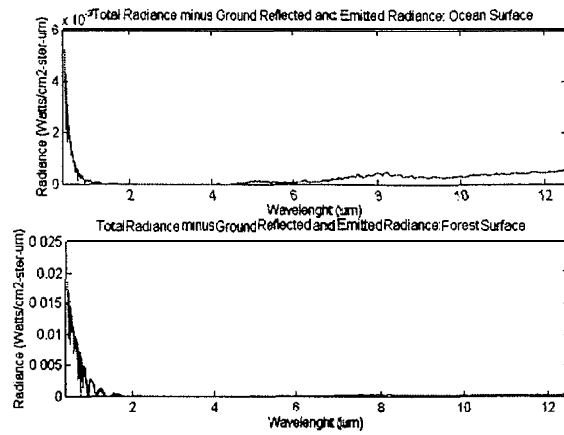Figure 3 Radiance due to Ground Reflection and Emission

Figure 4 Total Radiance

Figure 5 Radiance due to Scattering Effects